Astrocyte-derived lactoferrin reduces Aβ burden by promoting the interaction of p38 and PP2A in APP/PS1 transgenic mice

Yong-Gang Fan[1], Chuang Guo[2], Ling-Xiao Zhao[1], Ri-Le Ge[1], Zhong-Qiu Pang[2], Da-Long He[1], Hang Ren[1], Yan-Hui Zhang[1], and Zhan-You Wang[1]

[1]China Medical University
[2]Northeastern University

December 15, 2022

Abstract

Background and Purpose: Overexpression of astrocytic lactoferrin (Lf) was observed in the brains of Alzheimer's disease (AD) patients, whereas the role of astrocytic Lf in AD progression remains unexplored. In this study, we aimed to evaluate the effects of astrocytic Lf on AD progression. Experimental Approach: The APP/PS1 mice with astrocytes overexpressing human Lf were developed to evaluate the effects of astrocytic Lf on AD progression, and the N2a-sw cells were employed to further uncover the mechanism of astrocytic Lf on β-amyloid (Aβ) production. Key Results: Astrocytic Lf overexpression increased protein phosphatase 2A (PP2A) activity, and reduced amyloid precursor protein (APP) phosphorylation, Aβ burden and tau hyperphosphorylation in APP/PS1 mice. Mechanistically, astrocytic Lf overexpression promoted the astrocytic Lf secretion into neurons in APP/PS1 mice, and the conditional medium from astrocytes overexpressing Lf inhibited the p-APP(Thr668) expression in N2a-sw cells. Furthermore, the recombinant human Lf (hLf) also significantly enhanced PP2A activity and inhibited p-APP expression, while inhibitions of p38 or PP2A activities abrogated the hLf-induced p-APP downregulation in N2a-sw cells. Additionally, hLf promoted the interaction of p38 and PP2A via p38 activation, thereby enhancing PP2A activity; and low-density lipoprotein receptor-related protein 1 (LRP1) knockdown significantly reversed the hLf-induced p38 activation and p-APP downregulation. Conclusions and Implications: Our data suggested that astrocytic Lf promoted neuronal p38 activation via targeting to LRP1, subsequently promoting p38 binds to PP2A to enhance PP2A activity, which finally inhibited Aβ production via APP dephosphorylation. Therefore, promoting astrocytic Lf expression may be a potential strategy against AD.

Αστροςψτε-δεριεδ λαστοφερριν ρεδυςες Αβ βυρδεν βψ προμοτινγ τηε ιντεραστιον οφ π38 ανδ ΠΠ2Α ιν ΑΠΠ/ΠΣ1 τρανσγενις μιςε

Yong-Gang Fan[1, #], Chuang Guo[2, #], Ling-Xiao Zhao[1], Ri-Le Ge[1], Zhong-Qiu Pang[2], Da-Long He[1], Hang Ren[1], Yan-Hui Zhang[1], Zhan-You Wang[1, *]

[1] Key Laboratory of Medical Cell Biology of Ministry of Education, Key Laboratory of Major Chronic Diseases of Nervous System of Liaoning Province, Health Sciences Institute of China Medical University, Shenyang, 110122, China.

[2] College of Life and Health Sciences, Northeastern University, Shenyang, 110169, China.

[#] These authors contributed equally to this work.

[*]Correspondence and requests for materials should be addressed to Z.Y.W. (email: wangzy@cmu.edu.cn).

Running title: Lactoferrin against Alzheimer's disease

Background and Purpose: Overexpression of astrocytic lactoferrin (Lf) was observed in the brains of Alzheimer's disease (AD) patients, whereas the role of astrocytic Lf in AD progression remains unexplored. In this study, we aimed to evaluate the effects of astrocytic Lf on AD progression.

Experimental Approach: The APP/PS1 mice with astrocytes overexpressing human Lf were developed to evaluate the effects of astrocytic Lf on AD progression, and the N2a-sw cells were employed to further uncover the mechanism of astrocytic Lf on β-amyloid (Aβ) production.

Key Results: Astrocytic Lf overexpression increased protein phosphatase 2A (PP2A) activity, and reduced amyloid precursor protein (APP) phosphorylation, Aβ burden and tau hyperphosphorylation in APP/PS1 mice. Mechanistically, astrocytic Lf overexpression promoted the astrocytic Lf secretion into neurons in APP/PS1 mice, and the conditional medium from astrocytes overexpressing Lf inhibited the p-APP(Thr668) expression in N2a-sw cells. Furthermore, the recombinant human Lf (hLf) also significantly enhanced PP2A activity and inhibited p-APP expression, while inhibitions of p38 or PP2A activities abrogated the hLf-induced p-APP downregulation in N2a-sw cells. Additionally, hLf promoted the interaction of p38 and PP2A via p38 activation, thereby enhancing PP2A activity; and low-density lipoprotein receptor-related protein 1 (LRP1) knockdown significantly reversed the hLf-induced p38 activation and p-APP downregulation.

Conclusions and Implications: Our data suggested that astrocytic Lf promoted neuronal p38 activation via targeting to LRP1, subsequently promoting p38 binds to PP2A to enhance PP2A activity, which finally inhibited Aβ production via APP dephosphorylation. Therefore, promoting astrocytic Lf expression may be a potential strategy against AD.

Keywords

Alzheimer's disease; astrocytic lactoferrin; PP2A; p38; APP phosphorylation; β-amyloid

What is already known

Astrocytic Lf was overexpressed in the brains of AD patients, and supplemented with Lf could inhibit Aβ production via upregulating ADAM10 expression.

What this study adds

- Overexpression of Lf in astrocytes reduced Aβ burden via inhibiting Aβ production.
- The PP2A activity was modulated by the p38 activation-mediated interaction of p38 and PP2Ac.
- Astrocytes could secrete Lf to neurons to stimulate p38 activation by targeting LRP1, and finally promoting PP2A-mediated dephosphorylation of APP.

What is the clinical significance

Astrocytic Lf is a promising target to alleviate AD progression.

Ethics statement

This study was carried out in accordance with the recommendations of "Laboratory Animals-Guideline of welfare and ethics, The Ethics Committee for Medical Laboratory Animals of China Medical University" (the reference number: CMU2021430). The protocol was approved by The Ethics Committee for Medical Laboratory Animals of China Medical University.

Funding statement

This study was financially supported by the National Natural Science Foundation of China (92049106, 31970967), and a Project funded by China Postdoctoral Science Foundation (2021MD703901).

Author contributions

Y.G.F. performed most of the experiments and wrote the manuscript; L.X.Z. and R.L.G. contributed to experiments; Z.Q.P. and H. R. generated and validated the mouse model; D.L.H. and Y.H.Z. contributed

to the discussion; C. G. and Z.Y.W. designed the experiments and edited the manuscript. All authors have read and approved the final manuscript.

Competing interests

The authors declare that they have no competing interests.

Data availability statement

The data that support the findings of this study are available from the corresponding author upon reasonable request. Some data may not be made available because of privacy or ethical restrictions.

INTRODUCTION

Alzheimer's disease (AD) is the most common dementia worldwide, with no effective therapeutic strategies to date. The most characteristic neuropathology of AD is the extracellular fibrillar β-amyloid protein (Aβ) that aggregates to form senile plaques (SPs), which is highly associated with hyperphosphorylated tau protein, ectopic inflammatory stress and neuronal loss, *etc* . The successive cleavage of amyloid precursor protein (APP) by β-site APP cleavage enzyme 1 (BACE1) and γ-secretase is the main source of Aβ (Vassar et al., 1999). Furthermore, APP can also be cleaved by α-secretase (ADAM10) to constitute a nonamyloidogenic pathway (Sisodia, 1992). According to these observations, strategies for inhibiting Aβ production and promoting Aβ clearance from the brain were developed to alleviate AD progression. However, the clinical trials of BACE1 inhibitors failed, which may be ascribed to that the inhibitors didn't inhibit the expression or activity of BACE1, but elevated BACE1 expression by extending its half-life (Liu et al., 2019). Moreover, most of the clinical trials of Aβ monoclonal antibody drugs were terminated because of the poor efficacies and outstanding adverse events (Lu et al., 2020). Therefore, developing novel strategies for the treatment of AD is urged.

APP phosphorylation was elucidated to play a critical role in Aβ generation. When phosphorylation of APP at Thr668, the APP is a tendency to translocate to the endosomes where is an enrichment of BACE1, thus promoting the Aβ production; in contrast, mutation of APP at Thr668 or inhibition of p-APP(Thr668) expression decreased the Aβ production (Lee et al., 2003). Furthermore, a recent study also revealed that the phosphorylation of APP at Ser675 enhanced the Aβ production by promoting the meprin β-mediated APP-processing at the plasma membrane (Menon et al., 2019). These data suggest that inhibition of APP phosphorylation at specific sites is a promising strategy to repress Aβ production. Notably, the protein phosphatase 2A (PP2A) was known to dephosphorylation of APP at Thr668 (Shentu et al., 2018), and enhanced PP2A activity could effectively reduce the Aβ production by decreasing the p-APP expression (Hu et al., 2022). However, the activity of PP2A but not PP2A expression was significantly reduced in the brains of AD patients (Sontag and Sontag, 2014), suggesting that upregulation of PP2A activity is a hopeful strategy to relieve AD progression.

Lactoferrin (Lf), a secreted glycoprotein, is overexpressed in the astrocytes and microglia as well as neurons in the brains of elderly people and AD patients (Kawamata et al., 1993; Leveugle et al., 1994). Recently, the decreased salivary Lf was identified as a specific biomarker for AD (Gonzalez-Sanchez et al., 2020), while another study also declaimed that the Lf in saliva and cerebrospinal fluid was unchanged in the condition of AD (Gleerup et al., 2021). notably, non-parametric machine learning analysis on transcriptomic data from a large neuropathologically characterized patient cohort revealed that Lf is a key predictor of Aβ pathology (Tsatsanis et al., 2021). Our previous study revealed that exogenous Lf supplementation effectively reduced Aβ production through upregulating ADAM10 in APP/PS1 mice (Guo et al., 2017). A recent study also exerted beneficial actions of dietary Lf in J20 mice via inhibiting BACE1 expression and promoting Aβ clearance by astrocytes (Abdelhamid et al., 2020). Given that the overexpression of Lf in astrocytes was observed in the brains of AD patients (Kawamata et al., 1993), we speculated that the astrocytic Lf may have beneficial effects on AD progression. It is notable that Lf significantly activated p38 activation in MC3T3-E1 osteoblast cells (Liu et al., 2018), and p38 may possess a potential role in regulating the PP2A activity (Grethe and Porn-Ares, 2006), suggesting that the astrocytic Lf may regulate the Aβ production

via modulating PP2A-mediated APP dephosphorylation.

In this study, we investigated the roles of astrocytic Lf in AD progression. Our study revealed that overexpression of astrocytic Lf promoted the secretion of Lf from astrocytes, and Lf treatment significantly elevated the PP2A activity by promoting the interaction of p38 and PP2A to decrease APP phosphorylation; furthermore, overexpression of astrocytic Lf reduced the Aβ burden via increasing the PP2A-mediated APP dephosphorylation, resulting in the improvement of cognitive capacity in APP/PS1 mice. Thus, promoting astrocytic Lf expression may be a beneficial strategy for treating AD.

METHODS

2.1 Transgenic mice

The APPswe/PSEN1dE9 (APP/PS1) transgenic mice co-expressing human APPSwe and PS1-dE9 mutations with C57BL/6 background, were purchased from the Jackson Laboratory. The transgenic mice overexpressing human Lf (GenBank: BC015822.1) in astrocytes (Astro-Lf mice) in a background of C57BL/6 were generated by Cyagen Biosciences Inc. In brief, the pRP.ExBi-GFAP-Lf plasmid with GFAP promotor-driven human Lf cDNA expression was injected into the male pronucleus of fertilized eggs of C57BL/6 mice, the fertilized eggs were then transferred into the fallopian tube of pseudopregnant female mice to construct and screen the Astro-Lf mice. The Astro-Lf mice were crossed with the APP/PS1 mice to obtain the APP/PS1 mice with astrocytes overexpressing human Lf (APP/PS1/Lf mice). The DNA from tail biopsies were submitted to the polymerase chain reaction (PCR) to identify the different genotype mice. The following primers were used: Lf (human): forward, ATCGCCAGTCTAGCCCACTC and reverse, TCTCTTTATGCAGCTGACAGGA; Internal control: forward, ACTCCAAGGCCACTTATCACC and reverse, ATTGTTACCAACTGGGACGACA. All the mice were housed in cages with free access to a standard diet and distilled water under standard conditions (24 , 12 h light-dark cycle). Male mice at the age of 10 months old were submitted to animal behavioral tests and sacrificed for the biochemical analyses.

2.2 Tissue preparation

Mice were anesthetized with sodium pentobarbital (50 mg/kg, intraperitoneally), and subsequently transcardially perfused with physiological saline. Mice were sacrificed by decapitation, and the brains were immediately dissected in half on an ice-cold board. One was fixed in the 4% polyformaldehyde for morphological assessments, the other half was frozen at -80 °C for biochemical analyses.

Reagent

The hLf was purchased from Sigma-Aldrich (L4040), which was dissolved in physiological saline at the concentration of 25 mg/ml for the stock solution and stored at -80 °C.

2.4 Aβ42 ολιγομερ πρεπαρατιον

The Aβ42 oligomer was generated as our previous study (Fan et al., 2019). Briefly, the lyophilized Aβ42 peptide (ChinaPeptides, China) was dissolved in 1,1,1,3,3,3-hexafluoro-2-propanol (HFIP; Sigma, 105228) and divided into quarters before removing HFIP. The Aβ42 oligomer was obtained by incubating at 4 for 24 h in the F12 medium. Western blotting using the antibody against Aβ oligomer (Millipore, AB9234, 1: 1000) was performed to the quality control of the Aβ42 oligomer.

2.5 Primary astrocyte culture

The primary astrocytes were extracted according to our previous study with some modifications (Xu et al., 2022). In this study, wild-type (WT) mice and Astro-Lf mice were employed to obtain the primary astrocytes. Briefly, the newborn mice were sacrificed, and the cortexes were isolated and minced with forceps. Cortical tissues were further incubated with DMEM containing 0.25% trypsin-EDTA for 15 min at 37 °C. Dissociated cells were centrifuged at 500 *g* for 5 min and resuspended in DMEM containing 10% FBS and 1% penicillin/streptomycin. Cells were seeded into 75 cm^2 culture flasks and grown at 37°C in a 5% CO_2 incubator with a change of medium twice a week. After cell confluence, flasks were shaken in a rotator at

220 rpm for 6 h to purify astrocytes. Cells were treated with 10 μM cytosine arabinoside (Sigma, C1768) for 48 h to prevent the proliferation of other cell types, and the medium was replaced with DMEM containing 3% FBS and 0.15 mM dibutyryl cAMP (Sigma, D0267) to induce differentiation. Cells with GFAP-positive >95% were used for the following study. After the treatment of dibutyryl cAMP for 3 days, the medium was removed and changed to 1% FBS medium to further culture for 48 h. The medium was collected as the astrocytic conditional medium to treat the N2a-sw cells for 24 h or to enrich the medium proteins with acetone to detect the secreted Lf, and astrocytes were also collected for the western blot analysis.

2.6 Cell culture and treatment

The mouse neuroblastoma cells overexpressing the human APP695 Swedish mutation (K595N/M596L) (N2a-sw cells) was a gift from professor Huaxi Xu in Xiamen University. The N2a-sw cells (passage 8-15) were used for the in vitro studies. Cells were cultured in high glucose DMEM (Gibco, Carlsbad, CA) containing 10% FBS (Gibco, Carlsbad, CA), 100 U/ml penicillin (Sigma), 100 ug/ml streptomycin (Sigma) at 37 °C in a humidified atmosphere of 5% CO_2. Cells were seeded onto a six-well plate or slides for 36 h and subsequently starved in FBS free medium for 12 h. Cells were subsequently treated with Lf (0.05 mg/ml and 0.1 mg/ml) for 24 h, or co-treated with Lf (0.1 mg/ml) and p38 inhibitor SB203580 (MCE, 2 μM) or PP2A inhibitor calyculin A (CA, MCE, 0.5 nM) for 24 h, or co-treated with p38 inhibitor SB 203580 (MCE, 2 μM) and PP2A agonist DT-061 (MCE, 1 nM) or for 24 h. Cells were then harvested and analyzed.

2.7 p38 transfection

The p38-overexpressing lentiviruses (LV-p38) were generated by transfecting third-generation viral packaging plasmids (pRSV-Rv:VSVG:pMDLg/RRE, 5:3:2) and lentiviral vectors (p38-Flag) into HEK 293T cells. Briefly, 5×10^5 HEK 293T cells were co-transfected by 2 μg packaging plasmids and 2 μg lentiviral vectors. The virus supernatant was collected after 48 h transfection. N2a-sw cells were then incubated in the virus supernatant for 36 h, following selection with puromycin (Invivogen; 2 μg/ml). Generation of N2a-sw cells overexpressing p38-Flag was confirmed by western blotting.

2.8 LRP1 knockdown

The mouse LRP1-specific sense (5'-GGA GUC ACU UAC AUC AAU AUU-3') and antisense (5'-UAU UGA UGU AAG UGA CUC CUU-3') RNA oligonucleotides were synthesized by Hanbio Biotechnology Co., Ltd (Shanghai, China). The LRP1 siRNA were generated according to the manufacturer's instructions. Cells were transfected with LRP1 siRNA (50 nM) using GP-Transfect-mate (GenePharma, G04008) according to the manufacturer's specifications. Cells were further cultured for 48 h before treating with Lf (0.1 mg/ml) for 24 h.

2.9 Immunohistochemistry staining

Paraffin-embedded brains were sectioned at a thickness of 5 μm. Sections were then dewaxed and followed by antigen retrieval using L.A.B solution (Polyscience, Inc) for 20 min. After the blockage of goat serum for 30 min, the sections were incubated with rabbit anti-p-tau (Ser396) (Sigma, SAB4504557, 1: 100) overnight at 4 °C. Sections were subsequently incubated with biotinylated secondary antibodies for 1 h and third antibody for 30 min at room temperature, and further developed in DAB for 3 min. Finally, the sections were dehydrated and sealed. The images were captured by a light microscope (Leica, DM4000B).

2.10 Immunostaining

The mouse brains were cut on a cryostat (Leica, CM1850) at a thickness of 10 μm. A series of three equally spaced brain sections (˜1 mm apart) were used for each type of stain. The slides or cells were fixed with 4% paraformaldehyde for 10 min, followed by permeabilized with 0.2% Triton X-100 for 10 min at room temperature. After blockage with 5% BSA (Sigma-Aldrich) for 1 h, sections or cells were incubated with mouse anti-Aβ (Santa Cruz, sc-28365, 1: 400), rabbit anti-p-APP (Cell Signaling Technology, 6986, 1: 100), rabbit anti-human Lf (Abmart, T59526, 1: 100), mouse anti-GFAP (Cell Signaling Technology, 3670, 1: 200) and mouse anti-NeuN (Cell Signaling Technology, 94403, 1: 200) overnight at 4 °C. The secondary antibodies,

goat anti-rabbit-Ig G Alexa 555 (Themo Fisher Scientific, A32732, 1:400), goat anti-mouse-Ig G Alexa 555 (Themo Fisher Scientific, A21422, 1:400), goat anti-rabbit-Ig G Alexa 488 (Themo Fisher Scientific, A11008, 1:400) and goat anti-mouse-Ig G Alexa 488 (Themo Fisher Scientific, A32723, 1:400) were employed. Images of Aβ staining in the half mouse brains were captured by fluorescent microscope (Nikon, NI-SH-E), and the other images were obtained using a confocal laser microscope (Nikon, A1). The quantifications of the numbers and areas of Aβ-positive plaques, as well as the fluorescent intensities of Aβ and p-APP were both performed using Image J software. At least twenty-five cells were measured to evaluate the Aβ index and p-APP index in a single N2a-sw cell (Fan et al., 2019).

2.11 PP2A activity assay

The phosphatase activity of PP2A was evaluated using the PP2A activity detection kit (R&D Systems, DYC3309-2) according to the manufacturer's instructions. Briefly, the cortexes or cells were lysed in lysis buffer and centrifuged at 2000 *g* for 5 min. the protein concentrations were measured using a BCA kit. Subsequently, the samples were added to 96-well plates coated with antibody specific for the PP2Ac. After removing unbound stuff, a serine/threonine synthetic phosphopeptide substrate, which is dephosphorylated by active PP2A to generate free phosphate and unphosphorylated peptide, was added. The free phosphate was detected by a dye-binding assay using malachite green and molybdic acid after 30 min incubation. The phosphatase activity of PP2A was evaluated by calculating the rate of phosphate release.

2.12 Sandwich ELISA

For the detection of Aβ42 in the N2a-sw cell medium, the cell mediums were collected after the treatment of Lf (0.05 mg/ml and 0.1 mg/ml) for 24 h. The Aβ42 content was determined using Aβ42 kits (Invitrogen, HKB3544) according to the manufacturer's instructions. Absorbance values were recorded using a microplate reader at a wavelength of 450 nm.

2.13 Western blot

Cortexes or cells were lysed with RIPA buffer supplemented with protease inhibitor, NaF, PMSF and phosphatase inhibitor. The protein concentrations were determined using a BCA kit according to the manufacturer's instructions. Proteins were separated by SDS/PAGE and then transferred to PVDF membranes to incubated with rabbit anti-Lf (Millipore, 07-685, 1:1000; recognizes mouse and human Lf), rabbit anti-human Lf (Abmart, T59526, 1: 1000), rabbit anti-APP695 (Cell Signaling Technology, 2452, 1: 1000), rabbit anti-C-APP (Sigma, SAB4200535, 1:1000), rabbit anti-BACE1 (Abcam, ab183612, 1: 1000), rabbit anti-AMAD 10 (Cell Signaling Technology, 14194, 1: 1000), rabbit anti-presenilin-1 (PS1; Cell Signaling Technology, 5643, 1: 1000), mouse anti-soluble amyloid precursor α (sAPPα· Immuno-Biological Laboratories, 11088, 1: 500), mouse anti-soluble amyloid precursor β (sAPPβ· Immuno-Biological Laboratories, 10321, 1: 500), mouse anti-insulin-degrading enzyme (IDE; Santa Cruz, sc-514458, 1:500), goat anti-apolipoprotein E (APOE; Santa Cruz, sc-6384, 1: 500), rabbit anti-low-density lipoprotein receptor-related protein 1 (LRP1; Abcam, ab92544, 1: 8000), rabbit anti-advanced glycation end products (RAGE; Sigma, SAB2105049, 1: 1000), rabbit anti-Oligomer (Millipore, AB9234, 1: 1000), mouse anti-tau (Sigma, 577801, 1:5000), rabbit anti-p-tau (Thr181) (Cell Signaling Technology, 62672, 1: 2000), rabbit anti-p-tau (Ser202) (Cell Signaling Technology, 39357, 1: 2000), rabbit anti-p-tau (Thr231) (Cell Signaling Technology, 71429, 1: 2000), rabbit anti-p-tau (Ser396) (sigma, SAB4504557, 1: 2000), rabbit anti-p-tau (Ser404) (Cell Signaling Technology, 35834, 1: 2000), rabbit anti-glycogen synthase kinase 3α/β (GSK3α/β· Cell Signaling Technology, 5676, 1: 3000), rabbit anti-p-GSK3α/β (Ser21/9) (Cell Signaling Technology, 8566, 1: 4000), rabbit anti-p38 (Cell Signaling Technology, 8690, 1: 2000), rabbit anti-p-p38 (Cell Signaling Technology, 4511, 1: 2000), rabbit anti-cyclin-dependent kinase 5 (CDK5; Cell Signaling Technology, 14145, 1: 1000), rabbit anti-p-CDK5 (Cell Signaling Technology, 19051, 1: 1000), rabbit anti-PP2Ac (Cell Signaling Technology, 2038, 1: 1000), rabbit anti-p-Erk1/2 (Cell Signaling Technology, 4370, 1: 1000), rabbit anti-Erk1/2 (Cell Signaling Technology, 4695, 1: 1000) and mouse anti-β-actin (Sigma, A2228, 1: 10000) overnight at 4 °C. Membranes were washed with TBST and subsequently incubated with horseradish peroxidase (HRP)-labeled secondary antibodies for 1 h at room temperature. Enhanced chemiluminescence (ECL) kits (Tanon, 180-5001) and Chem Doc

XRS with Quantity One software (Bio-Rad, 5500) were applied to detect blots. Data from the bands were determined using Image J software.

2.14 Immunoprecipitation assay

After the treatment of Lf and/or SB203580 for 24 h, the N2a-sw cells were solubilized in NP40 buffer supplemented with protease inhibitor and PMSF, one part of the protein extracts were used as the input control, and the rest (˜1 mg) was incubated with rabbit anti-PP2Ac antibody (Cell Signaling Technology, 2038) (another extract from untreated N2a-sw cells was incubated with IgG as the negative control) overnight at 4 °C, and followed by precipitation with protein A-beads (Thermo Fisher Scientific, 10001D) for 4 h at 4 °C. The beads were washed and added with 50 μl sample buffer, the mixture was boiled for 5 min and sedimented, and the supernatant was used for western blot analysis.

2.15 Morris water maze

The Morris water maze (MWM) was performed as described in our previous study with some modifications (Fan et al., 2019). Briefly, mice at the age of 10 months old were trained for 2 days and subsequently tested for 5 days using MWM. The mice were trained 3 times a day for 2 days to find the visible platform (5 cm dia.) above the water, and then were tested 3 trails a day for 5 days to find the hidden platform (1 cm below the water surface). A total of 1 min was given for the mice to find the platform. The escape latency and the path length during MWM were recorded using SMART 3.0 software to evaluate their spatial learning scores. For the probe trail test, 24 h after the last trail of the hidden platform test, the platform was removed, and the number of times that the mice crossed the platform region during 1 min was recorded by the SMART 3.0 software.

2.16 Statistical analysis

All the experiments and analyses are conducted in a blinded manner. All values are presented as the mean ± SEM. Statistical analysis was determined by Student's t -test (two-group comparison), one-way analysis of variance (ANOVA) or two-way ANOVA followed by the Bonferroni's post hoc test using GraphPad Prism 8.0. A P value of < 0.05 was considered as significant statistically throughout this study.

RESULTS

3.1 Οερεξπρεσσιον οφ Λφ ιν αστροςψτες ρεδυςες Αβ βυρδεν ανδ ιμπροες ςογνιτιε αβιλιτψ ιν ΑΠΠ/ΠΣ1 μιςε

The MWM was a classical animal behavior experiment to assess the spatial learning and memory capacity of mice. In the visible platform tests, the Astro-Lf mice exhibited a shorter escape latency and path length compared to the other gene-type mice, whereas the WT mice, APP/PS1 mice and APP/PS1/Lf mice had no significant difference in the escape latency (Fig. 1A) or path length (Fig. 1B), indicating that overexpression of Lf in astrocytes may promote the vision or motility in WT mice, neither in APP/PS1 mice. However, in the hidden platform tests, the APP/PS1/Lf mice spent less time (Fig. 1C) and travelled shorter lengths (Fig. 1D-E) than APP/PS1 mice to search the hidden platform on day 5. Moreover, APP/PS1/Lf mice exhibited more crossing times than those of APP/PS1 mice (Fig. 1F), suggesting that astrocytic Lf overexpression rescued the cognitive impairments of APP/PS1 mice.

After the end of animal behavior tests, mice were sacrificed and the brains were harvested. Immunostaining results showed significant reductions in the number of Aβ plaque and the area of Aβ plaque in both the cortexes and hippocampus of APP/PS1/Lf mice compared to those in APP/PS1 mice (Fig. 1G-I). The decreased Aβ loads in the APP/PS1/Lf mice were also confirmed by immunoblotting as shown in Fig. 1J. These data suggested that astrocytic Lf overexpression effectively reduced the Aβ burden in APP/PS1 mouse brains, and subsequently enhanced the cognitive capacity of APP/PS1 mice.

3.2 Overexpression of Lf in astrocytes promotes the Lf secretion into neurons

To uncover the mechanism of decreased Aβ burden in APP/PS1/Lf mice, we examined the expression levels

of Lf in different gene-type mice. Immunoblotting showed that although the expressions of Lf in WT mouse brains and APP/PS1 mouse brains remain similar (Fig. 2A), the Lf content in APP/PS1/Lf mouse brains was significantly elevated compared to that in APP/PS1 mouse brains (Fig. 2B). Furthermore, the mouse primary astrocytes from Astro-Lf mice exhibited significant increases in Lf expression and Lf secretion compared to the primary astrocytes from WT mice (Fig. 2C), suggesting that overexpression of Lf in astrocytes promoted the Lf secretion from astrocytes. Similarly, the robust expression of human Lf was observed in the APP/PS1/Lf mouse brains (Fig. 2D), which was accompanied by strong immunostaining of human Lf in the NeuN-positive cells (Fig. 2E), suggesting that overexpression of Lf in astrocytes promoted the Lf secretion into neurons.

3.3 Overexpression of Lf in astrocytes inhibits APP phosphorylation in APP/PS1 mice

Given that the astrocytes could secrete Lf into neurons (Fig. 2), we, therefore, evaluated the key proteins involved in APP-processing. As shown in Fig. 3A, the APP phosphorylation at Thr668 was dramatically inhibited in the APP/PS1/Lf mice compared to the APP/PS1 mice, whereas the critical enzymes for APP-processing such as ADAM10, BACE1 and PS1 remained similar. Immunostaining also showed that the p-APP expression was highly associated with Aβ deposition, and was reduced in the neurons in APP/PS1/Lf mouse cortex (Fig. 3B, Supplementary Fig. 1). Inhibition of p-APP expression was demonstrated to repress the BACE1-mediated Aβ production (Lee et al., 2003). As expected, the production of BACE1-mediated APP cleavage, sAPPβ, was considerably reduced in APP/PS1/Lf mice (Fig. 3C), indicating that the APP amyloidogenic pathway was inhibited by the overexpression of Lf in astrocytes in APP/PS1 mice.

Aβ homeostasis is also modulated by the capacity of Aβ clearance in the brain. We, therefore, analyzed the Aβ efflux protein LRP1 and its ligand APOE, the Aβ-degrading enzyme IDE, and the Aβ influx protein RAGE. Although APOE was significantly increased in the Astro-Lf mice compared to the WT mice, the expressions of APOE in APP/PS1/Lf mice and APP/PS1 mice were similar (Fig. 3D). Additionally, the RAGE expressions were unchanged in the different gene type mice, while overexpression of Lf in astrocytes effectively rescued the decreased expression of LRP1 and IDE in APP/PS1 mice (Fig. 3D). These data suggested that overexpression of Lf in astrocytes inhibited Aβ burden via repressing APP phosphorylation and promoting Aβ clearance in APP/PS1 mouse brains.

3.4 Overexpression of Lf in astrocytes enhances PP2A activity and reduces tau phosphorylation in APP/PS1 mouse brains

APP phosphorylation is modulated by several enzymes such as CDK5, GSK3α/β and PP2A (Keeney et al., 2012; Lee et al., 2003; Shentu et al., 2018). Our results revealed that the level of p-CDK5 was reduced, and p-GSK3α/β (Ser21/9) was upregulated, while p-ERK1/2 was unaltered, in the APP/PS1/Lf mice compared to that in APP/PS1 mice (Fig. 4A). Interestingly, the p-p38 expression was considerably upregulated in APP/PS1/Lf mice, which was accompanied with the increased activity of PP2A in the APP/PS1/Lf mice compared to that in APP/PS1 mice despite the expressions of PP2Ac (the catalytic subunit of PP2A) remained similar in the different gene type mouse brains (Fig. 4B-C). These data suggested that overexpression of Lf in astrocytes may inhibit APP phosphorylation via suppressing CDK5 and GSK3α/β activities and increasing PP2A activity in APP/PS1 mouse brains.

Notably, tau phosphorylation is regulated by the activities of CDK5, GSK3α/β and PP2A (Keeney et al., 2012). The phosphorylations of tau at Thr181 and Ser404 were significantly increased in Astro-Lf mice compared to WT mice, and the phosphorylations of tau at Thr181, Ser396 and Ser404 were significantly reduced in the APP/PS1/Lf mice compared to those in APP/PS1 mice (Fig. 4D-E), suggesting that overexpression of Lf in astrocytes also effectively inhibited the tau phosphorylation in APP/PS1 mouse brains.

3.5 hLf inhibits APP phosphorylation via p38 and PP2Ac interaction-mediated upregulation of PP2A activity

To further unveil the mechanism of p-APP downregulation in the APP/PS1/Lf mouse brains, the mouse primary astrocytes and N2a-sw cells were employed in the following studies. Our data revealed that Aβ42

oligomers treatment significantly upregulated the Lf expression in primary astrocytes from WT mice, and also promote Lf secretion from astrocytes (Fig. 5A), suggesting that astrocytic Lf may have a role in regulating Aβ metabolism. Indeed, the conditional astrocytic medium from Astro-Lf mice significantly repressed the p-APP expression in N2a-sw cells (Fig. 5B), indicating that the astrocytes may secrete Lf to directly inhibit the p-APP expression in neurons since the elevated Lf content was observed in the medium of astrocytes from Astro-Lf mice (Fig. 2C). To further elucidate our hypothesis, we employed hLf for the following studies. The hLf was reported to reduce Aβ production via upregulating ADAM10 in the N2a-sw cells in our previous study (Guo et al., 2017), therefore, we focused on the effect of hLf on p-APP expression in this study. As shown in Fig. 5C-D, the p-APP expression was reduced, which was coincident with the downregulations of sAPPβ expression and Aβ42 production after hLf treatment in the N2a-sw cells. Furthermore, the immunostaining data (Fig. 5E) revealed that the p-APP fluorescent intensity was positively correlated with the Aβ fluorescent intensity in the control cells (Fig. 5E1) and hLf-treated cells (Fig. 5E1); and the p-APP fluorescent intensity was downregulated (Fig. 5E4), which was accompanied by the decreased Aβ fluorescent intensity (Fig. 5E3) in the hLf-treated cells, suggesting that hLf effectively reduced the Aβ production via inhibition of p-APP expression. Importantly, the p-p38 expression was dramatically upregulated, while the expressions of p-CDK5, p-GSK3α/β, and PP2Ac were unchanged in the hLf-treated N2a-sw cells (Fig. 5F). Nevertheless, the PP2A activity was also elevated in the hLf-treated N2a-sw cells (Fig. 5G), indicating that hLf treatment may increase the APP dephosphorylation via upregulation of PP2A activity, and this action may be associated with the activation of p38.

To verify that hLf-induced p-APP downregulation is in a p38 activation-dependent manner, the p38 inhibitor SB203580 was employed to treat the N2a-sw cells. As shown in Fig. 5H, inhibition of p38 activity abrogated the hLf treatment-induced p-APP downregulation, suggesting that hLf treatment inhibited p-APP expression needs p38 activation. Interestingly, inhibition of p38 considerably increased the p-APP expression (Fig. 5H), while activation of PP2A by its agonist DT-061 completely reversed this circumstance in N2a-sw cells (Fig. 5I), indicating that p38 may regulate the p-APP expression in a PP2A activity-dependent manner. As expected, the PP2A antagonist CA also clearly rescued the p-APP expression in hLf-treated N2a-sw cells (Fig. 5J). These data suggested that hLf promoted APP dephosphorylation via enhancing PP2A activity through p38 activation. Next, we asked how the p38 activation regulates the hLf-induced enhancement of PP2A activity. As shown in Fig. 5K, hLf treatment increased the interaction of p38 and PP2Ac, while inhibition of p38 activity significantly abrogated this effect in N2a-sw cells. Furthermore, the changes in the interaction of p38 and PP2Ac after hLf and/or SB203580 treatment were highly coincidence with the changes in the PP2A activities (Fig. 5L), suggesting that hLf treatment enhanced the PP2A activity via increasing the interaction of p38 and PP2Ac by promoting p38 activation. To further elucidate that p38 interacts with PP2Ac to regulate PP2A activity, p38 was introduced into the N2a-sw cells. As shown in Fig. 5M-N, overexpression of p38 significantly increased the PP2A activity without changing the expression of PP2Ac. Moreover, overexpression of p38 slightly reduced the APP expression, but sharply inhibited the phosphorylation of APP at Thr668 and the production of sAPPβ in N2a-sw cells (Fig. 5O). Together, our data suggested that hLf inhibited APP phosphorylation at Thr668 via enhancing PP2A activity by activation of p38.

The actions of astrocyte-derived Lf on neurons may be mediated by the neuronal receptors of Lf. LRP1 was reported to be a putative receptor of Lf (Tang et al., 2010), we, therefore, knocked down LRP1 in N2a-sw cells (Fig. 5P). Our data suggested that LRP1 silence significantly abrogated the hLf-induced p38 activation, and also rescued the hLf-induced downregulation of p-APP in N2a-sw cells (Fig. 5Q), indicating that hLf treatment promoted p38 activation-mediated downregulation of p-APP expression partly via targeting to its neuronal receptor LRP1.

DISCUSSION

Lf is overexpressed in the glial cells and neurons of the elderly person and AD patients (Kawamata et al., 1993; Leveugle et al., 1994), while, to date, the functions of Lf in different cell types remain unexplored. Our recent study exerted that astrocytic Lf knockout impaired the neuronal dendritic complexity and cognitive ability

via decreasing cholesterol production during early life in mice (Xu et al., 2022), suggesting the important roles of astrocytes in regulating neuronal functions. Several studies revealed that supplements with Lf effectively retarded AD progression (Abdelhamid et al., 2020; Guo et al., 2017). In this study, the human Lf gene was firstly knocked in the astrocytes in the APP/PS1 mice, and the results showed that overexpression of Lf reduced the Aβ burden via enhancing PP2A activity by the activation of p38 in APP/PS1 mice. Hence, promoting astrocytic Lf expression may be a promising strategy for treating AD.

The current strategies for treating AD are suffering severe challenges because the clinical trials of Aβ monoclonal antibody drugs and BACE1 inhibitors are almost failed. Therefore, the other targets for regulating Aβ production have gained great attention in the following studies. APP was previously demonstrated to be a potential target to inhibit Aβ production, however, APP is an important membrane receptor that involves in the signaling transductions in neurons (Deyts et al., 2016), and APP knockout significantly impairs neuronal excitability and synaptic plasticity (Lee et al., 2020; Weyer et al., 2011). Therefore, decreasing neuronal APP expression may lead to serious side effects. Notably, APP phosphorylation is an important step for Aβ production. Phosphorylation of APP at Tyr682 by Fyn tyrosine kinase promoted the APP translocated into acidic neuronal compartments where it is processed to generate Aβ (Iannuzzi et al., 2020). Phosphorylation of APP at Ser675 also altered the balance of APP-processing through increasing meprin β-mediated and decreasing α-secretase-mediated APP cleavage at the plasma membrane (Menon et al., 2019). Additionally, phosphorylation of APP at Thr668 promoted the APP transfer to the endosome where is cleaved by the BACE1 and subsequently promoted Aβ generation (Lee et al., 2003). In this study, astrocytic Lf overexpression inhibited the phosphorylation of neuronal APP at Thr668, thereby diminishing Aβ burden in APP/PS1 mice. Our previous study revealed that intranasal treatment of Lf repressed the Aβ production via upregulating ADAM10 expression in APP/PS1 mice (Guo et al., 2017). Similar to our previous study, dietary supplemented with Lf also reduced the Aβ production in J20 transgenic mice, whereas its mechanism involved the BACE1 inhibition, but not the ADAM10 upregulation (Abdelhamid et al., 2020). Furthermore, Lf intake was shown to reduce the contents of Aβ, tau, and oxidative damage markers in the serum of AD patients, and enhance the cognitive functions of AD patients (Mohamed et al., 2019). These studies suggested that the different source of Lf may have different molecular mechanisms against AD. Surely, our current study showed a significant decrease in APP phosphorylation, but not ADAM10 and BACE1 in APP/PS1/Lf mice, suggesting that the astrocyte-derived Lf may preferentially inhibited Aβ production via decreasing neuronal APP phosphorylation in the condition of AD.

The Aβ burden is also modulated by the capacity of Aβ clearance. Endothelial LRP1 could interact with Aβ and promote Aβ transcytosis across the blood-brain barrier, thus enhancing Aβ efflux (Storck et al., 2016). Furthermore, the neuronal LRP1 could also assist the uptake of Aβ by neurons to degradation without influencing the Aβ-degrading enzymes (Kanekiyo et al., 2013). Our study revealed that astrocytic Lf overexpression rescued the downregulation of LRP1 in APP/PS1 mice, suggesting the enhancement of Aβ clearance in the APP/PS1/Lf mouse brains. The IDE expression was also upregulated in APP/PS1/Lf mouse brains. IDE is an Aβ-degrading enzyme that is predominately secreted by the astrocytes via an autophagy-based unconventional secretory pathway (Son et al., 2016). A previous study revealed that Lf promoted the secretion of astrocytic IDE to degrade Aβ (Abdelhamid et al., 2020), we, therefore, suggested that astrocytic Lf overexpression may promote Aβ degradation via directly promoting the astrocytic IDE secretion in APP/PS1 mice. Notably, LRP1 and IDE were both reduced in the APP/PS1 mice compared to the WT mice, suggesting that Aβ may directly reduce the expressions of LRP1 and IDE. Therefore, whether the astrocyte-derived Lf upregulated the expressions of LRP1 and IDE is ascribed to reduced Aβ burden in APP/PS1/Lf mice merits further investigation. Nevertheless, we may conclude that astrocytic Lf overexpression could promote Aβ clearance by enhancing the expressions of LRP1 and IDE in APP/PS1 mice.

Hyperphosphorylation of tau is also a prominent hallmark of AD, it can impede the microtube assembly and impair the cellular cargo transport, subsequently leading to neuronal dysfunction and neuronal loss (Xia et al., 2021). Activations of CDK5 and GSK3α/β promote tau phosphorylation, while PP2A own the opposite effect through its phosphatase activity (Castro-Alvarez et al., 2014). Astrocytic Lf overexpression inhibited

the activities of CDK5 and GSK3α/β and increase the PP2A activity, thus decreasing tau phosphorylation in APP/PS1 mice. Of note, PP2A is also a critical regulator of APP phosphorylation, activation of PP2A activity effectively reduces the Aβ production via dephosphorylation of APP at Thr668 (Hu et al., 2022). The PP2A activities were elevated in the APP/PS1/Lf mouse brains and hLf-treated N2a-sw cells, suggesting that Lf may inhibit Aβ production via promoting PP2A-mediated APP dephosphorylation. Increasing evidence exerted that p38 activation may play an important role in regulating PP2A activity (Chiou et al., 2022; Grethe and Porn-Ares, 2006). Activation of p38 was reported to enhance the PP2A activity in tumor necrosis factor α (TNFα)-treated endothelial cells (Grethe and Porn-Ares, 2006). In addition, activation of p38 was also reported to stimulate the PP2A-mediated dephosphorylation of cAMP response element binding protein (CREB) (Chiou et al., 2022), and the mechanism may be ascribed to the p38 activation-induced phosphorylation of PP2Ac at Tyr307 (Hsiao et al., 2020). However, the PP2A activity evaluated using the PP2A (Tyr307) monoclonal antibodies is suffering great challenges since those antibodies are not specific for phosphorylated Tyr307 but instead are hampered by PP2Ac phosphorylation at Thr304 or methylation at Leu309 (Frohner et al., 2020; Mazhar et al., 2020). Therefore, the mechanism regarding p38 activation-induced enhancement of PP2A activity should be re-interpreted. Interestingly, p38 was verified as a partner of PP2A, and the interaction of p38 and PP2A involved in the stem cell factor-induced cardiac stem cell migration (Wang et al., 2017) and oxidative stress-induced DNA damage response (Guillonneau et al., 2016). The p38 activation was found in the APP/PS1/Lf mice and hLf-treated N2a-sw cells; furthermore, inhibition of p38 activity significantly reduced the interaction of p38 and PP2Ac, and also abrogated the hLf-induced interaction of p38 and PP2Ac; in addition, the alternations in the interaction of p38 and PP2Ac after hLf and/or SB203580 treatment were coincident with changes in the activities of PP2A, indicating that p38 activity regulated the interaction of p38 and PP2Ac, thus directly influenced the PP2A activity. Indeed, overexpression of p38 effectively upregulated the PP2A activity, further reinforcing our conclusion that p38 interacts with PP2Ac to enhance the PP2A activity. Taken together, our study firstly revealed that astrocyte-derived Lf inhibited APP phosphorylation via enhancing PP2A activity by promoting p38 activation-induced interaction of p38 and PP2Ac.

The p38 was proposed to be a downstream target of Lf since Lf treatment could effectively promote osteoblast cell proliferation and differentiation by stimulating the activation of p38 (Liu et al., 2018; Zhang et al., 2014). However, as the putative receptor of Lf, LRP1 did not implicate the Lf-induced p38 activation in osteoblast cells (Tang et al., 2010; Zhang et al., 2014). In contrast, our study revealed that LRP1 knockdown largely abrogated the hLf-induced p38 activation, and subsequently reversed hLf-mediated p-APP downregulation in N2a-sw cells, indicating that the hLf-indued p38 activation was partly in a LRP1-dependent manner in N2a-sw cells. Consistent with our results, the p38 activation was also observed in a LRP1-dependent manner in the Aβ42-treated neurons and astrocytes (Ma et al., 2016; Yang et al., 2015), suggesting the LRP1-p38 axis may be a conserved signaling pathway in neurons. Collectively, we may conclude that astrocyte-derived Lf may stimulate p38 activation via targeting neuronal LRP1 and subsequently reduce the neuronal p-APP expression.

CONCLUSION

our data firstly confirmed that overexpression of Lf in astrocytes promoted the secretion of Lf from astrocytes, which subsequently bound to its neuronal receptor LRP1 and trigged the activation of p38, followed by elevation of PP2A activity via stimulating the interaction of p38 and PP2Ac, and finally diminished Aβ production through dephosphorylation of APP at Thr668 in neurons (Fig. 6). Hence, promoting astrocytic Lf expression may be an attractive strategy to alleviate AD progression.

References

Abdelhamid, M., Jung, C.G., Zhou, C., Abdullah, M., Nakano, M., Wakabayashi, H., Abe, F., and Michikawa, M. (2020). Dietary Lactoferrin Supplementation Prevents Memory Impairment and Reduces Amyloid-beta Generation in J20 Mice. *J Alzheimers Dis* , *74* , 245-259.

Castro-Alvarez, J.F., Uribe-Arias, S.A., Mejia-Raigosa, D., and Cardona-Gomez, G.P. (2014). Cyclin-

dependent kinase 5, a node protein in diminished tauopathy: a systems biology approach. *Front Aging Neurosci* , *6* , 232.

Chiou, J.T., Huang, C.H., Wu, T.H., Wang, L.J., Lee, Y.C., Huang, P.W., and Chang, L.S. (2022). CREB/Sp1-mediated MCL1 expression and NFkappaB-mediated ABCB1 expression modulate the cytotoxicity of daunorubicin in chronic myeloid leukemia cells. *Toxicol Appl Pharmacol* , *435* , 115847.

Deyts, C., Thinakaran, G., and Parent, A.T. (2016). APP Receptor? To Be or Not To Be. *Trends Pharmacol Sci* , *37* , 390-411.

Fan, Y.G., Guo, T., Han, X.R., Liu, J.L., Cai, Y.T., Xue, H., Huang, X.S., Li, Y.C., Wang, Z.Y., and Guo, C. (2019). Paricalcitol accelerates BACE1 lysosomal degradation and inhibits calpain-1 dependent neuronal loss in APP/PS1 transgenic mice. *EBioMedicine* , *45* , 393-407.

Frohner, I.E., Mudrak, I., Schuchner, S., Anrather, D., Hartl, M., Sontag, J.M., Sontag, E., Wadzinski, B.E., Preglej, T., Ellmeier, W.*, et al.* (2020). PP2AC Phospho-Tyr(307) Antibodies Are Not Specific for this Modification but Are Sensitive to Other PP2AC Modifications Including Leu(309) Methylation. *Cell Rep* ,*30* , 3171-3182 e3176.

Gleerup, H.S., Jensen, C.S., Hogh, P., Hasselbalch, S.G., and Simonsen, A.H. (2021). Lactoferrin in cerebrospinal fluid and saliva is not a diagnostic biomarker for Alzheimer's disease in a mixed memory clinic population. *EBioMedicine* , *67* , 103361.

Gonzalez-Sanchez, M., Bartolome, F., Antequera, D., Puertas-Martin, V., Gonzalez, P., Gomez-Grande, A., Llamas-Velasco, S., Herrero-San Martin, A., Perez-Martinez, D., Villarejo-Galende, A.*, et al.* (2020). Decreased salivary lactoferrin levels are specific to Alzheimer's disease. *EBioMedicine* , *57* , 102834.

Grethe, S., and Porn-Ares, M.I. (2006). p38 MAPK regulates phosphorylation of Bad via PP2A-dependent suppression of the MEK1/2-ERK1/2 survival pathway in TNF-alpha induced endothelial apoptosis. *Cell Signal* , *18* , 531-540.

Guillonneau, M., Paris, F., Dutoit, S., Estephan, H., Beneteau, E., Huot, J., and Corre, I. (2016). Oxidative stress disassembles the p38/NPM/PP2A complex, which leads to modulation of nucleophosmin-mediated signaling to DNA damage response. *FASEB J* ,*30* , 2899-2914.

Guo, C., Yang, Z.H., Zhang, S., Chai, R., Xue, H., Zhang, Y.H., Li, J.Y., and Wang, Z.Y. (2017). Intranasal Lactoferrin Enhances alpha-Secretase-Dependent Amyloid Precursor Protein Processing via the ERK1/2-CREB and HIF-1alpha Pathways in an Alzheimer's Disease Mouse Model. *Neuropsychopharmacology* , *42* , 2504-2515.

Hsiao, P.C., Chang, J.H., Lee, W.J., Ku, C.C., Tsai, M.Y., Yang, S.F., and Chien, M.H. (2020). The Curcumin Analogue, EF-24, Triggers p38 MAPK-Mediated Apoptotic Cell Death via Inducing PP2A-Modulated ERK Deactivation in Human Acute Myeloid Leukemia Cells. *Cancers (Basel)* , *12* .

Hu, W., Wang, Z., Zhang, H., Mahaman, Y.A.R., Huang, F., Meng, D., Zhou, Y., Wang, S., Jiang, N., Xiong, J.*, et al.* (2022). Chk1 Inhibition Ameliorates Alzheimer's Disease Pathogenesis and Cognitive Dysfunction Through CIP2A/PP2A Signaling. *Neurotherapeutics* .

Iannuzzi, F., Sirabella, R., Canu, N., Maier, T.J., Annunziato, L., and Matrone, C. (2020). Fyn Tyrosine Kinase Elicits Amyloid Precursor Protein Tyr682 Phosphorylation in Neurons from Alzheimer's Disease Patients. *Cells* , *9* .

Kanekiyo, T., Cirrito, J.R., Liu, C.C., Shinohara, M., Li, J., Schuler, D.R., Shinohara, M., Holtzman, D.M., and Bu, G. (2013). Neuronal clearance of amyloid-beta by endocytic receptor LRP1. *J Neurosci* ,*33* , 19276-19283.

Kawamata, T., Tooyama, I., Yamada, T., Walker, D.G., and McGeer, P.L. (1993). Lactotransferrin immunocytochemistry in Alzheimer and normal human brain. *Am J Pathol* , *142* , 1574-1585.

Keeney, J.T., Swomley, A.M., Harris, J.L., Fiorini, A., Mitov, M.I., Perluigi, M., Sultana, R., and Butterfield, D.A. (2012). Cell cycle proteins in brain in mild cognitive impairment: insights into progression to Alzheimer disease. *Neurotox Res* , *22* , 220-230.

Lee, M.S., Kao, S.C., Lemere, C.A., Xia, W., Tseng, H.C., Zhou, Y., Neve, R., Ahlijanian, M.K., and Tsai, L.H. (2003). APP processing is regulated by cytoplasmic phosphorylation. *J Cell Biol* ,*163* , 83-95.

Lee, S.H., Kang, J., Ho, A., Watanabe, H., Bolshakov, V.Y., and Shen, J. (2020). APP Family Regulates Neuronal Excitability and Synaptic Plasticity but Not Neuronal Survival. *Neuron* , *108* , 676-690 e678.

Leveugle, B., Spik, G., Perl, D.P., Bouras, C., Fillit, H.M., and Hof, P.R. (1994). The iron-binding protein lactotransferrin is present in pathologic lesions in a variety of neurodegenerative disorders: a comparative immunohistochemical analysis. *Brain Res* , *650* , 20-31.

Liu, L., Lauro, B.M., Ding, L., Rovere, M., Wolfe, M.S., and Selkoe, D.J. (2019). Multiple BACE1 inhibitors abnormally increase the BACE1 protein level in neurons by prolonging its half-life. *Alzheimers Dement* , *15* , 1183-1194.

Liu, M., Fan, F., Shi, P., Tu, M., Yu, C., Yu, C., and Du, M. (2018). Lactoferrin promotes MC3T3-E1 osteoblast cells proliferation via MAPK signaling pathways. *Int J Biol Macromol* , *107* , 137-143.

Lu, L., Zheng, X., Wang, S., Tang, C., Zhang, Y., Yao, G., Zeng, J., Ge, S., Wen, H., Xu, M.*, et al.* (2020). Anti-Abeta agents for mild to moderate Alzheimer's disease: systematic review and meta-analysis.*J Neurol Neurosurg Psychiatry* , *91* , 1316-1324.

Ma, K.G., Lv, J., Hu, X.D., Shi, L.L., Chang, K.W., Chen, X.L., Qian, Y.H., Yang, W.N., and Qu, Q.M. (2016). The p38 mitogen-activated protein kinase signaling pathway is involved in regulating low-density lipoprotein receptor-related protein 1-mediated beta-amyloid protein internalization in mouse brain. *Int J Biochem Cell Biol* ,*76* , 75-86.

Mazhar, S., Leonard, D., Sosa, A., Schlatzer, D., Thomas, D., and Narla, G. (2020). Challenges and Reinterpretation of Antibody-Based Research on Phosphorylation of Tyr(307) on PP2Ac. *Cell Rep* , *30* , 3164-3170 e3163.

Menon, P.K., Koistinen, N.A., Iverfeldt, K., and Strom, A.L. (2019). Phosphorylation of the amyloid precursor protein (APP) at Ser-675 promotes APP processing involving meprin beta. *J Biol Chem* ,*294* , 17768-17776.

Mohamed, W.A., Salama, R.M., and Schaalan, M.F. (2019). A pilot study on the effect of lactoferrin on Alzheimer's disease pathological sequelae: Impact of the p-Akt/PTEN pathway. *Biomed Pharmacother* ,*111* , 714-723.

Shentu, Y.P., Huo, Y., Feng, X.L., Gilbert, J., Zhang, Q., Liuyang, Z.Y., Wang, X.L., Wang, G., Zhou, H., Wang, X.C.*, et al.* (2018). CIP2A Causes Tau/APP Phosphorylation, Synaptopathy, and Memory Deficits in Alzheimer's Disease. *Cell Rep* , *24* , 713-723.

Sisodia, S.S. (1992). Beta-amyloid precursor protein cleavage by a membrane-bound protease. *Proc Natl Acad Sci U S A* , *89* , 6075-6079.

Son, S.M., Cha, M.Y., Choi, H., Kang, S., Choi, H., Lee, M.S., Park, S.A., and Mook-Jung, I. (2016). Insulin-degrading enzyme secretion from astrocytes is mediated by an autophagy-based unconventional secretory pathway in Alzheimer disease. *Autophagy* , *12* , 784-800.

Sontag, J.M., and Sontag, E. (2014). Protein phosphatase 2A dysfunction in Alzheimer's disease. *Front Mol Neurosci* , *7* , 16.

Storck, S.E., Meister, S., Nahrath, J., Meissner, J.N., Schubert, N., Di Spiezio, A., Baches, S., Vandenbroucke, R.E., Bouter, Y., Prikulis, I.*, et al.* (2016). Endothelial LRP1 transports amyloid-beta(1-42) across the blood-brain barrier. *J Clin Invest* , *126* , 123-136.

Tang, L., Wu, J.J., Ma, Q., Cui, T., Andreopoulos, F.M., Gil, J., Valdes, J., Davis, S.C., and Li, J. (2010). Human lactoferrin stimulates skin keratinocyte function and wound re-epithelialization. *Br J Dermatol* , *163* , 38-47.

Tsatsanis, A., McCorkindale, A.N., Wong, B.X., Patrick, E., Ryan, T.M., Evans, R.W., Bush, A.I., Sutherland, G.T., Sivaprasadarao, A., Guennewig, B.*, et al.* (2021). The acute phase protein lactoferrin is a key feature of Alzheimer's disease and predictor of Abeta burden through induction of APP amyloidogenic processing. *Mol Psychiatry* , *26* , 5516-5531.

Vassar, R., Bennett, B.D., Babu-Khan, S., Kahn, S., Mendiaz, E.A., Denis, P., Teplow, D.B., Ross, S., Amarante, P., Loeloff, R.*, et al.* (1999). Beta-secretase cleavage of Alzheimer's amyloid precursor protein by the transmembrane aspartic protease BACE. *Science* ,*286* , 735-741.

Wang, Y., Xia, Y., Kuang, D., Duan, Y., and Wang, G. (2017). PP2A regulates SCF-induced cardiac stem cell migration through interaction with p38 MAPK. *Life Sci* , *191* , 59-67.

Weyer, S.W., Klevanski, M., Delekate, A., Voikar, V., Aydin, D., Hick, M., Filippov, M., Drost, N., Schaller, K.L., Saar, M.*, et al.*(2011). APP and APLP2 are essential at PNS and CNS synapses for transmission, spatial learning and LTP. *EMBO J* , *30* , 2266-2280.

Xia, Y., Prokop, S., and Giasson, B.I. (2021). "Don't Phos Over Tau": recent developments in clinical biomarkers and therapies targeting tau phosphorylation in Alzheimer's disease and other tauopathies. *Mol Neurodegener* , *16* , 37.

Xu, S.F., Pang, Z.Q., Fan, Y.G., Zhang, Y.H., Meng, Y.H., Bai, C.Y., Jia, M.Y., Chen, Y.H., Wang, Z.Y., and Guo, C. (2022). Astrocyte-specific loss of lactoferrin influences neuronal structure and function by interfering with cholesterol synthesis. *Glia* .

Yang, W.N., Ma, K.G., Qian, Y.H., Zhang, J.S., Feng, G.F., Shi, L.L., Zhang, Z.C., and Liu, Z.H. (2015). Mitogen-activated protein kinase signaling pathways promote low-density lipoprotein receptor-related protein 1-mediated internalization of beta-amyloid protein in primary cortical neurons. *Int J Biochem Cell Biol* , *64* , 252-264.

Zhang, W., Guo, H., Jing, H., Li, Y., Wang, X., Zhang, H., Jiang, L., and Ren, F. (2014). Lactoferrin stimulates osteoblast differentiation through PKA and p38 pathways independent of lactoferrin's receptor LRP1.*J Bone Miner Res* , *29* , 1232-1243.

Figure legends

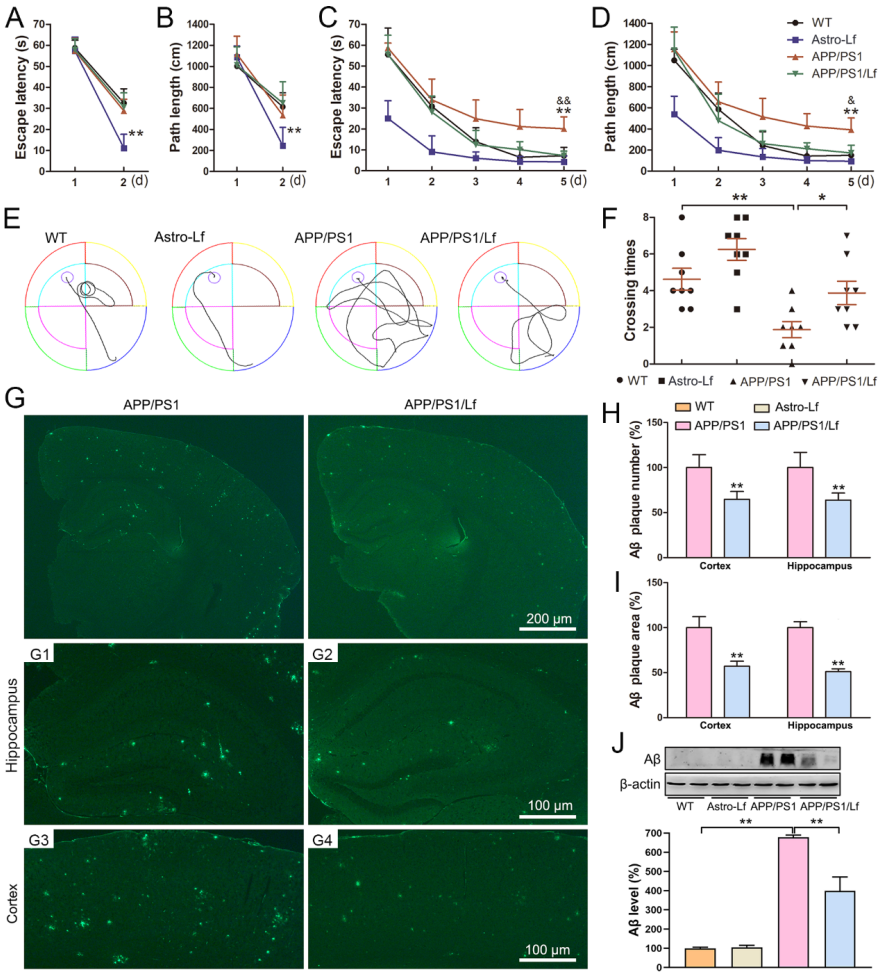

Φιγυρε 1. Οερεξπρεσσιον οφ Λφ ιν αστροςψτες ρεδυςες Αβ βυρδεν ανδ ιμπροες ςογνιτιε αβιλιτψ ιν ΑΠΠ/ΠΣ1 μιςε. The male mice at 10-months-old were submitted to MWM tests with 2 days of visible platform training, and 5 days of hidden platform tasting, as well as a probe trial after 24 h of the last hidden platform test. The numbers of mice used in this study as follow: WT = 8, Astro-Lf = 8, APP/PS1 = 8, APP/PS1/Lf = 8. (A-B) The escape latencies and path lengths in the visible platform tests. (C-D) The escape latencies and path lengths at day 5 in the hidden platform tests were shortened in the WT mice and APP/PS1/Lf mice, compared to those in APP/PS1 mice. * showing WT*vs* APP/PS1, & showing APP/PS1 *vs* APP/PS1/Lf; Two-way ANOVA followed by the Bonferroni's post hoc test. (E) Graphs showing representative paths at day 5 in the hidden platform tests. (F) In the probe trials, the WT mice and APP/PS1/Lf mice exhibited more crossing times than APP/PS1 mice. Two-way ANOVA followed by the Bonferroni's post hoc test. (G) Immunostaining showing the Aβ plaques in the mouse brains, the magnified images of hippocampus and cortexes are respectively presented in G1, G2 and G3, G4. n = 5. (H-I) Overexpression of Lf in astrocytes decreased both the numbers and areas of Aβ plaque in APP/PS1 mice. n = 4; Student's t -test. (J) The expression levels of Aβ were reduced in APP/PS1/Lf mice compared to the APP/PS1 mice. n = 6; Two-way ANOVA followed by the Bonferroni's post hoc test.$^{\&}P < 0.05$,$^{\&\&}P < 0.01$; $^{*}P < 0.05$, $^{**}P < 0.01$.

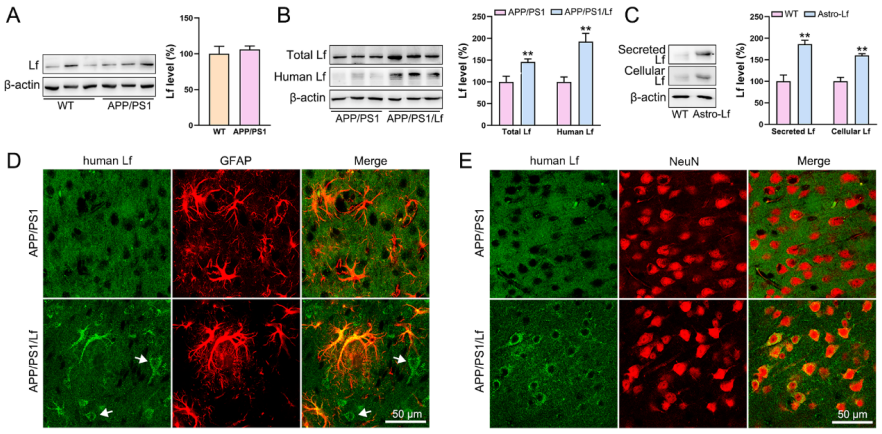

Figure 2. Overexpression of Lf in astrocytes promotes Lf secretion into neurons. (A) The expression of Lf was unchanged between the WT mouse brains and APP/PS1 mouse brains at the age of 10-months old. n = 6; Student's t -test. (B) The contents of total Lf (mouse Lf and human Lf) and human Lf were increased in APP/PS1/Lf mouse brains. n = 6; Student's t -test. (C) The contents of cellular and secreted Lf were increased in the mouse primary astrocytes from Astro-Lf mice. n = 5; Student's t -test. (D) The human Lf was overexpressed in the astrocytes from APP/PS1/Lf mouse brains. n = 5. (E) Human Lf was observed in the NeuN-positive cells in APP/PS1/Lf mouse brains. n = 5. $^{**}P < 0.01$.

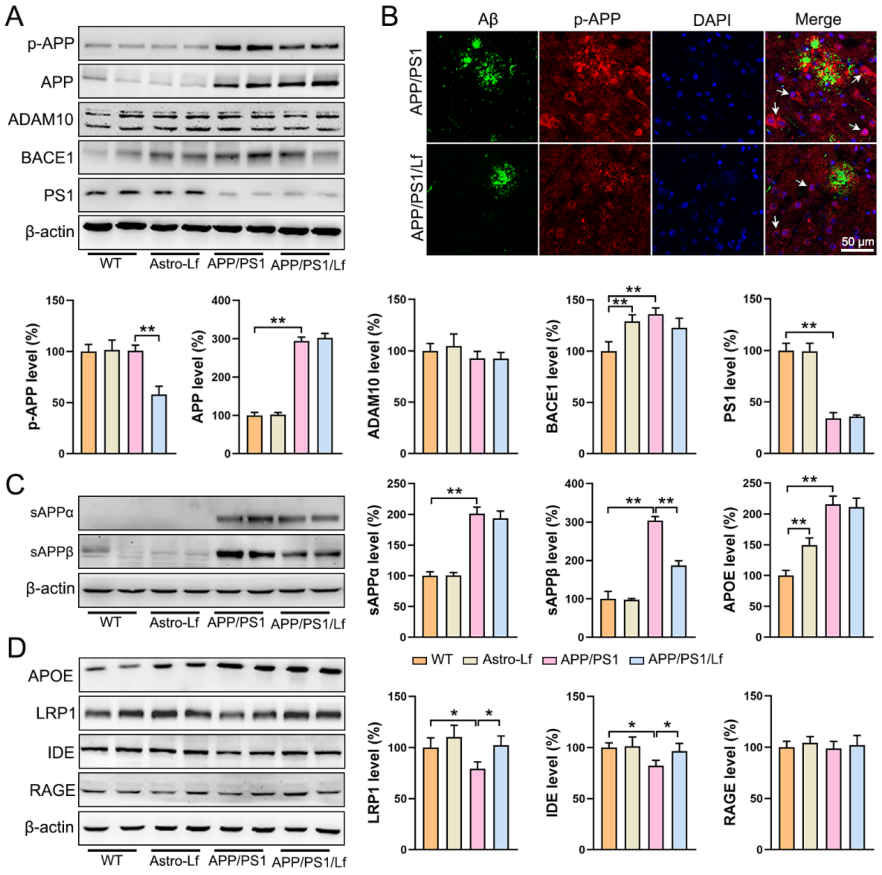

Figure 3. Overexpression of Lf in astrocytes inhibits APP phosphorylation in APP/PS1 mice. (A) The expression of p-APP (Thr668) was downregulated, while the expressions of APP, BACE1, ADAM10, and PS1 remained similar in APP/PS1/Lf mice compared to APP/PS1 mice. n = 6; Two-way ANOVA followed by the Bonferroni's post hoc test. (B) Double immunostaining showing the reductions of p-APP expression in the Aβ plaques and neurons in APP/PS1/Lf mouse cortex. White arrows indicate the neurons. n = 5. (C) Overexpression of Lf in astrocytes reduced the expression of sAPPβ, but did not affect the expression of sAPPα in APP/PS1 mice. n = 6; Two-way ANOVA followed by the Bonferroni's post hoc test. (D) Overexpression of Lf in astrocytes promoted the expression of APOE in WT mice, and reversed the downregulation of LRP1 and IDE in APP/PS1 mice. n = 6; Two-way ANOVA followed by the Bonferroni's post hoc test. $*P < 0.05$, $**P < 0.01$.

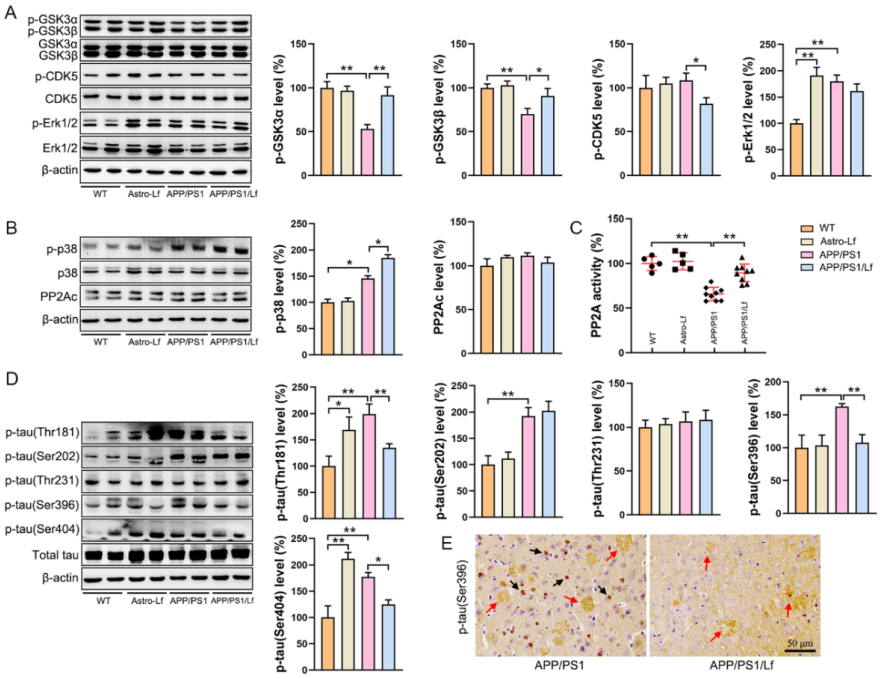

Figure 4. Overexpression of Lf in astrocytes enhances PP2A activity and reduces tau phosphorylation in APP/PS1 mouse brains. (A-B) The expressions of p-GSK3α/β (21/9) and p-p38 were increased, and the p-CDK5 was decreased, and the expressions of GSK3α/β, CDK5, p38, p-Erk1/2, Erk1/2 and PP2Ac were unchanged in APP/PS1/Lf mice compared to that in APP/PS1 mice. n = 6; Two-way ANOVA followed by the Bonferroni's post hoc test. (C) Overexpression of Lf in astrocytes elevated the activity of PP2A in APP/PS1 mice. (D) The phosphorylations of tau at Thr181 and Ser404 were upregulated in Astro-Lf mice compared to WT mice, whereas overexpression of Lf in astrocytes reversed the upregulated phosphorylation of tau at Thr18, Ser396 and Ser404 in APP/PS1 mice. n = 6; Two-way ANOVA followed by the Bonferroni's post hoc test. (E) Immunochemistry staining showing the decreased p-tau (Ser396) intensity in APP/PS1/Lf mouse cortex. n = 5. $*P < 0.05$, $**P < 0.01$.

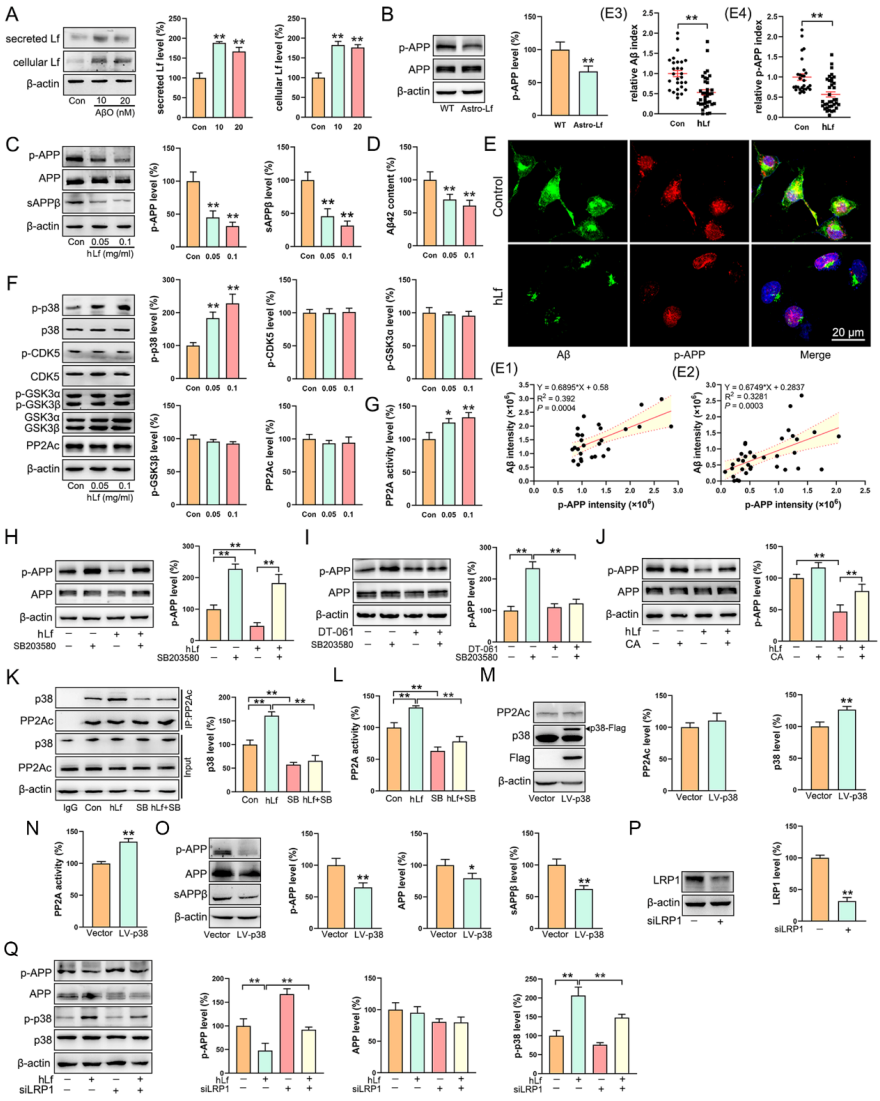

Figure 5. hLf inhibits APP phosphorylation via p38 and PP2Ac interaction-mediated upregulation of PP2A activity. (A) Aβ oligomer treatment increased the expression and secretion of Lf in the mouse primary astrocytes from WT mice. n = 5; one-way ANOVA. (B) Conditional astrocytic medium from Astro-Lf mice inhibited p-APP expression in N2a-sw cells. n = 3; Student's *t* -test. (C) hLf treatment reduced the expressions of p-APP and sAPPβ, but not APP in N2a-sw cells. n = 5; one-way ANOVA. (D) hLf treatment diminished the Aβ42 content in the medium. n = 5; one-way ANOVA. (E) Double immunostaining showing the fluorescent intensities of Aβ and p-APP in control N2a-sw cells and hLf-treated N2a-sw cells. The Aβ intensities were both positively correlated with p-APP intensities in control N2a-sw cells (E1) and hLf-treated N2a-sw cells (E2), and the intensities of Aβ (E3) and p-APP (E4) were both decreased in hLf-treated N2a-sw cells. n > 25; Student's *t* -test. (F) hLf treatment increased the expression of p-p38 but had no effects on the expressions of p38, p-CDK5, CDK5, p-GSK3α/β, GSK3α/β and PP2Ac in N2a-sw cells. n = 5; one-way ANOVA. (G) The PP2A activity was increased in hLf-treated N2a-sw cells. n = 5; one-way ANOVA. (H) Inhibition of p38 activity promoted p-APP expression, and also abrogated hLf-induced downregulation of p-APP in N2a-sw cells. n = 5; Two-way ANOVA followed by the Bonferroni's post hoc test. (I) Activation of PP2A activity rescued the p38 inhibition-induced upregulation of p-APP in N2a-sw cells. n = 5; Two-way ANOVA followed by the Bonferroni's post hoc test. (J) Inhibition of PP2A activity

abrogated hLf-induced downregulation of p-APP in N2a-sw cells. n = 5; Two-way ANOVA followed by the Bonferroni's post hoc test. (K) hLf treatment induced the interaction of PP2Ac and p38, while inhibition of p38 activity inhibited the interaction of PP2Ac and p38, and also abrogated the hLf-induced interaction of PP2Ac and p38 in N2a-sw cells. n = 5; Two-way ANOVA followed by the Bonferroni's post hoc test. (L) Inhibition of p38 activity reduced the PP2A activity and abrogated the hLf-induced upregulation of PP2A activity in N2a-sw cells. n = 5; Two-way ANOVA followed by the Bonferroni's post hoc test. (M-N) Overexpression of p38 enhanced the PP2A activity without changing the expression of PP2Ac in N2a-sw cells. n = 5; Student's t -test. (O) Overexpression of p38 slightly reduced the APP expression, but sharply decreased the expressions of p-APP and sAPPβ in N2a-sw cells. n = 5; Student's t -test. (P) LRP1 siRNA effectively knocked down the expression of LRP1 in N2a-sw cells. n = 3; Student's t -test. (Q) LRP1 silence largely inhibited the hLf-induced upregulation of p-p38 and subsequently rescued the hLf-induced downregulation of p-APP in N2a-sw cells. n = 5; Two-way ANOVA followed by the Bonferroni's post hoc test. $^{*}P < 0.05$, $^{**}P < 0.01$.

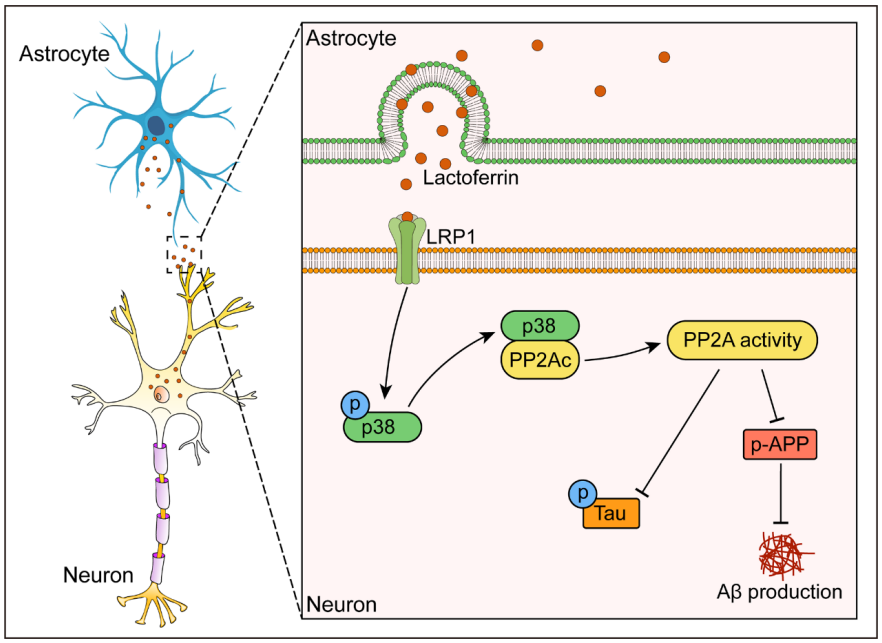

Figure 6. Schematic summarizing the findings from this study. Overexpression of astrocytic Lf promoted neuronal p38 activation via targeting to LRP1, subsequently promoting p38 binds to PP2Ac to enhance PP2A activity, which not only inhibited tau phosphorylation but also reduced Aβ production via APP dephosphorylation.